AGU PUBLICATIONS

JGR

Journal of Geophysical Research: Solid Earth

RESEARCH ARTICLE
10.1002/2017JB014469

Special Section:
Slow Slip Phenomena and Plate Boundary Processes

Key Points:
- We present an improved detection scheme coupling repeating earthquakes and GPS analysis
- We detect two previously unknown SSEs in Boso Peninsula that occurred in 2005 and 2010
- The recurrence time of the SSE is around 2.4 years

Supporting Information:
- Supporting Information S1
- Data Set S1
- Data Set S2

Correspondence to:
B. Gardonio,
blandine.gardonio@gmail.com

Citation:
Gardonio, B., Marsan, D., Socquet, A., Bouchon, M., Jara, J., Sun, Q., & Campillo, M. (2018). Revisiting slow slip events occurrence in Boso Peninsula, Japan, combining GPS data and repeating earthquakes analysis. *Journal of Geophysical Research: Solid Earth*, *123*, 1502–1515. https://doi.org/10.1002/2017JB014469

Received 23 MAY 2017
Accepted 29 NOV 2017
Accepted article online 5 DEC 2017
Published online 8 FEB 2018

Revisiting Slow Slip Events Occurrence in Boso Peninsula, Japan, Combining GPS Data and Repeating Earthquakes Analysis

B. Gardonio[1], D. Marsan[1], A. Socquet[2], M. Bouchon[2], J. Jara[2], Q. Sun[2], N. Cotte[2], and M. Campillo[2]

[1]University Grenoble Alpes, University Savoie Mont Blanc, CNRS, IRD, IFSTTAR, ISTerre, Chambéry, France, [2]University Grenoble Alpes, University Savoie Mont Blanc, CNRS, IRD, IFSTTAR, ISTerre, Grenoble, France

Abstract Slow slip events (SSEs) regularly occur near the Boso Peninsula, central Japan. Their time of recurrence has been decreasing from 6.4 to 2.2 years from 1996 to 2014. It is important to better constrain the slip history of this area, especially as models show that the recurrence intervals could become shorter prior to the occurrence of a large interplate earthquake nearby. We analyze the seismic waveforms of more than 2,900 events ($M \geq 1.0$) taking place in the Boso Peninsula, Japan, from 1 April 2004 to 4 November 2015, calculating the correlation and the coherence between each pair of events in order to define groups of repeating earthquakes. The cumulative number of repeating earthquakes suggests the existence of two slow slip events that have escaped detection so far. Small transient displacements observed in the time series of nearby GPS stations confirm these results. The detection scheme coupling repeating earthquakes and GPS analysis allow to detect small SSEs that were not seen before by classical methods. This work brings new information on the diversity of SSEs and demonstrates that the SSEs in Boso area present a more complex history than previously considered.

1. Introduction

The Boso Peninsula, Japan, is located on the Okhotsk plate above two subducting slabs: the Pacific (PAC) Plate plunges westward at depth, with the Philippine Sea Plate (PHS) subducting to the west-northwest just above it (Figure 1). This area is well known for the occurrence of several slow slip events (SSEs) along the top interface of PHS at shallow depth (between 10 and 30 km), in 1983, 1990, 1996, 2002, 2007, March 2011, October 2011, and 2014. These SSEs have a clear signature on geodetic measurements with a moment magnitude between 6.4 and 6.6 (Hirose et al., 2012, 2014; Ozawa et al., 2003; Sagiya, 2004).

The SSEs, whose sources have been estimated from surface GPS displacement inversion, ruptured the same characteristic patch (Hirose et al., 2012, 2014; Ozawa et al., 2003; Sagiya, 2004). In all cases, these SSEs have always been accompanied by swarm-like seismicity located at the northern downdip edge of this patch (Hirose et al., 2012; Ozawa et al., 2007), likely triggered by the slow slip event (Hirose et al., 2014).

The first three SSEs (in 1983, 1990, and 1996) occurred quasiperiodically. However, the recurrence interval has then been shown to decrease from 6.4 to 2.2 years from 1996 to 2014 (Ozawa, 2014). Shortening of SSEs recurrence intervals can be linked to a variety of processes: (i) long-term increase of the regional stressing rate, as evidenced by seismicity studies in this region (Marsan et al., 2017; Reverso et al., 2016); (ii) slow, long-term seismic decoupling, which would in effect result also in an increase of the local seismicity rate as observed (Marsan et al., 2017); (iii) afterslip of large earthquakes; (iv) or other external stress perturbations, as magma injection (Tu & Heki, 2014). In Boso area, no large events susceptible of impacting the recurrence interval of SSEs occurred before the Tohoku earthquake. Magma injection is very unlikely too. Furthermore, numerical friction models have shown that the recurrence intervals of SSEs could become shorter when a large interplate earthquake is about to occur nearby (Matsuzawa et al., 2010; Mitsui, 2015). It is thus necessary to better constrain the slip history of this area for seismic risk mitigation. Geodetically resolved SSEs broke a patch with nearly the same area, suggesting a simple physical process that breaks the same patch and has the same magnitude (Hirose et al., 2012, 2014; Ozawa et al., 2003; Sagiya, 2004).

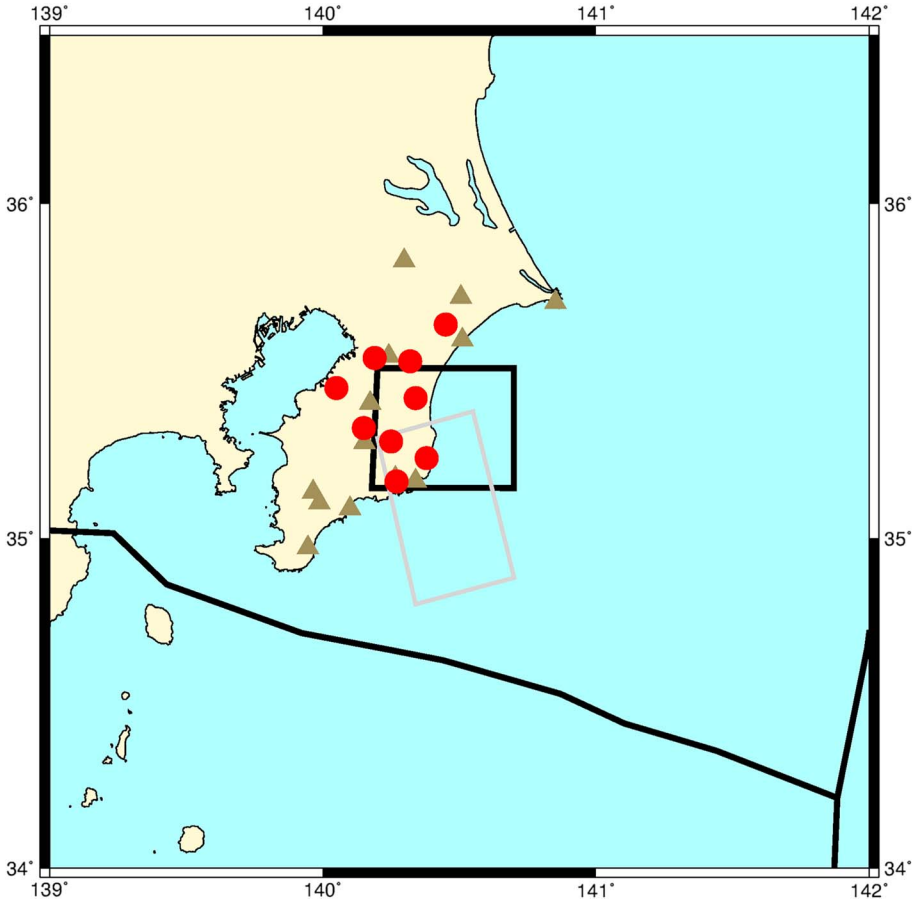

Figure 1. Tectonic settings of the Boso Peninsula. The brown triangles and red dots give the location of the seismic and GPS stations, respectively, used in this study. We analyze repeating earthquakes occurring in the black rectangle, which contains most swarm-like seismicity triggered during known SSEs. The broken lines show the depth contours of the plate interface of the PHS (Ishida, 1992). The white stars indicate the location of $M \geq 6$ earthquakes that occurred in 2005, 2011 and 2012. The focal mechanism of the 2005 Choshi earthquake is shown.

Since there exists an instrumental limit for detection, smaller SSEs could have escaped detection, so that the actual complexity of the process relieving tectonic stress in this area could actually be underestimated. We therefore wonder whether there could exist smaller SSEs in Boso area, or whether the SSEs are really characteristic in time, space, and slip. This would directly impact on the recurrence interval and thus on the possibility of having a large earthquake in the near future.

To answer these fundamental questions, we investigate slip episodes on the subduction interface by the joint analysis of repeating earthquakes (REs) and GPS time series. Indeed, REs are earthquakes that break a common asperity with nearly identical rupture lengths. These asperities are close to a velocity-strengthening (i.e., creeping) fault zone that slips to host SSEs. The evolution with time of the REs occurrence rate can thus give information on stress interactions between asperities, changes in creeping rate, or complexity in the rupture process (Bouchon et al., 2011; Lengliné & Marsan, 2009; Nadeau & McEvilly, 1999; Schaff et al., 1998). In this study, we focus on this sensitivity to changes in creeping rate. In order to establish the relationship between REs occurrence rate and transient deformation episodes, we analyze the distributions of REs in time and space and compare them to trends and transients in the GPS data after removing seasonal signals and the common modes. The combination of these observations allows to identify two SSEs, unknown so far, that are smaller in magnitude and/or lateral extension than the ones already know. In order to better characterize these two previously unknown events, we compare them to the 2007, March and October 2011, and 2014 SSEs that were also accompanied by a swarm-like seismicity. They occurred during the time lapse of our analysis and were largely studied (Hirose et al., 2012, 2014; Ozawa et al., 2007). The aim of this study is thus to assess how the

two most useful observables at hand (surface displacements by GPS and repeating waveforms) can be used to their limits to tell us something about the hidden slow slip events in Boso, in a complex context where no tectonic tremor exists.

2. Data and Methods

2.1. GPS Data Analysis

2.1.1. Daily cGPS Processing

The data of the entire GPS Earth Observation NETwork in Japan (GEONet), together with 44 IGS sites worldwide (International Global Navigation Satellite Systems (GNSS) Service for Geodynamics, http://igscb.nasa.jpl.org), were processed over the period 1994–2013 following a double-difference approach. Each day, the data set was divided into subnetworks of 40 stations including two tie stations near the middle of each subnetwork and no station used more than twice (for example, for day 365 of year 2009, we have 34 subnetworks for 1385 stations included in the processing). The 24 h sessions were reduced to daily estimates of station positions using the GAMIT 10.6 software (Herring et al., 2010), choosing the ionosphere-free combination and fixing the ambiguities to integer values. We use precise orbits from the International GNSS Service for Geodynamics, precise EOPs (Earth Orientation Parameters) from the IERS (International Earth Rotation and Reference Systems Service) bulletin B, IGS tables to describe the phase centers of the antennas, FES2004 (Lyard et al., 2006) ocean-tidal loading corrections, as well as atmospheric loading corrections (tidal and nontidal). We estimated one tropospheric zenith delay parameter every 2 h and one couple of horizontal tropospheric gradients per 24 h session, using the Vienna Mapping Function (VMF1, Boehm et al., 2006), to map the tropospheric delay in zenithal direction, with a priori ZHD (Zenithal Hydrostatic Delay) evaluated from pressure and temperature values from the VMF1 grids. Daily solutions were combined using the GLOBK software in a "regional stabilization" approach. Coordinate time series were then generated and mapped into the ITRF2014 reference frame (Altamimi et al., 2016) by applying Helmert transforms to adjust IGS stations coordinates to those defined in the ITRF in a least square iterative process.

2.1.2. Time Series Analysis and Identification of Transient Movements

To study transient deformation in the area of Boso, we followed a similar approach as in Socquet et al. (2017) on nine GPS stations, summarized hereafter. In order to avoid major coseismic offsets in our time series, we selected data from 9 August 2004 to 10 March 2011. Annual and semiannual signals were removed from the time series, as well as the long-term constant deformation associated with interseismic loading, by fitting a linear regression together with a pair of sinusoids terms. Jumps associated with documented equipment changes were also estimated. The 46 stable stations (i.e., not affected by local transient signal), located within a distance range of 50–150 km from the Boso SSEs' source region, were used to calculate and remove the regional common-mode noise. This procedure reduced significantly the scatter in our time series. In order to image transient signals present in our time series, we computed the average velocity variations of the obtained detrended and denoised time series, by fitting a linear regression in a 15 day sliding window.

2.2. Repeating Earthquakes Analysis

Repeating earthquakes (REs) are earthquakes that break a common asperity with nearly identical rupture lengths. These particular seismic events have been identified in California, most notably on the Parkfield segment of the San Andreas Fault (Nadeau et al., 1995), in Japan (Matsuzawa et al., 2002), including the Kanto region (Gardonio et al., 2015; Kimura et al., 2006), and in other parts of the world (e.g., Bouchon et al., 2011; Chen et al., 2007). REs have been hypothesized to be driven by the surrounding aseismic slip (Ellsworth & Beroza, 1995; Igarashi et al., 2003; Nadeau & McEvilly, 1999). Thus, they can be used to assess changes in creeping rate. In Boso, REs have been studied after the 2011 Tohoku-oki earthquake to evidence the existence of a SSE in March of that year, 2 days after the megathrust earthquake (Kato et al., 2014).

We analyze the waveforms of all $M \geq 1.0$, depth < 60 km earthquakes from April 2004 to November 2015, that are located in the Boso area ($35.51° \geq$ latitude $\geq 35.15°$ and $140.70° \geq$ longitude $\geq 140.18°$) as listed in the Japan Meteorological Agency (JMA) catalog. In total, we study 2,986 earthquakes recorded at 13 stations (Figure 1), elaborating on the method developed in Got et al. (1994) and Lengliné and Marsan (2009) and applied in Gardonio et al. (2015). We compute both the mean coherency and the cross correlation between all pairs of earthquakes at common stations for several frequency bands (1–4, 3–12, 5–20, 7–28, 9–36, and 11–44 Hz) on a 512 sample-long window initially centered on the *P* wave arrival. We keep the frequency band that gives the highest coherency and cross-correlation values. The coherency is defined as the smoothed cross

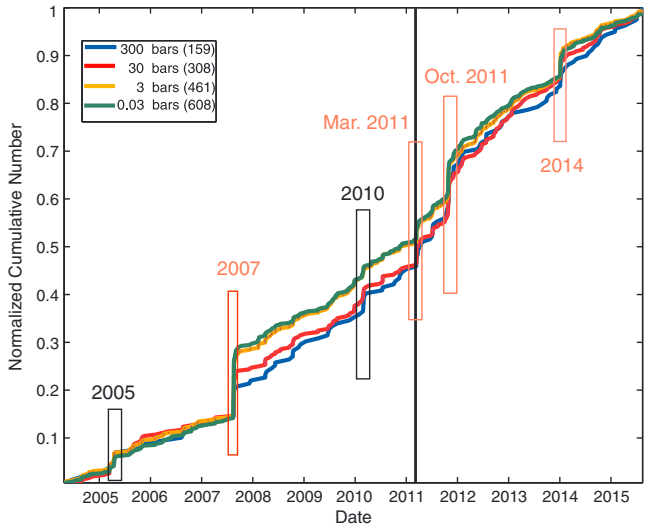

Figure 2. Normalized cumulative number of REs depending on the stress drop value used to calculate the rupture radii. The total number is given in brackets in the legend. The overall trend is independent of the stress drop. Only the number of REs is affected by the value of the stress drop (see text for more details). Known SSEs are shown with red rectangles, as they trigger transient activity of REs; we identify two potential new SSEs, as shown with the black rectangles, in 2005 and 2010. The vertical line marks the date of the 2011 *M*9.0 Tohoku earthquake.

spectrum normalized by the smoothed autospectra of each signal as $C_{xy}(\nu) = \frac{\overline{X(\nu)Y^*(\nu)}}{\sqrt{\overline{X(\nu)X^*(\nu)}}\sqrt{\overline{Y(\nu)Y^*(\nu)}}}$ with $X(\nu)$: Fourier transform of x and X^*, the complex conjugate of X. Smoothing is done by averaging over five consecutive frequency samples. Time delays are also computed in the same frequency bands using both coherency and cross correlation. Time delays are estimated with an uncertainty of half a sample (0.005 s) which corresponds to an error of 35 m at a wave velocity of 7 km/s. We then select all earthquake pairs characterized by a mean coherency greater than 0.99 for at least one station. In order to remove outliers, we reject time delays that differ by more than 0.01 s (one sample) when comparing time delay estimates based on both coherency and correlation. The kept time delays are then used to compute the relative coordinates of all the earthquakes within a group of multiplets (Got et al., 1994; Got & Okubo, 2003). We use the NIED (National Research Institute for Earth Science and Disaster Prevention) velocity model (Ukawa et al., 1984) and the NonLinLoc algorithm (Lomax et al., 2009) to compute the *P* wave arrival time, the azimuth, and the takeoff angle of every event. For two earthquakes to be repeating instances of a nearly identical rupture, we require $d < \max\{L_1, L_2\}$ with d, the distance between the two events; L_1, L_2 their rupture radii, calculated with $L = (7M_o/16\Delta\sigma)^{1/3}$ (Eshelby, 1957), for a $\Delta\sigma = 30$ bar stress drop; and M_o the seismic moment. We tested different values of stress drop (0.03, 3, and 300 bars) to explore the sensitivity of the results on this quantity (Figure 2). The stress drop value impacts the total number of REs (608, 461, and 159, respectively) which decreases when the stress drop increases. At a low stress drop, the rupture areas are large; thus, more events are gathered in a group than at a higher stress drop where the rupture size is smaller. The cumulative number of REs remains the same using different values of stress drop without any effect on the existence and resolution of transient episodes. Variations in REs occurrence rate are mostly unaffected by changes in the stress drop value, hence in the rupture dimension. This is important as we will use (in section 3) the most significant increases in REs rate as markers of the occurrence of SSEs using a stress drop of 30 bars.

Several studies have shown that the magnitude of REs that are located on the same asperity can vary with time in Japan where the Kamishi sequence presents an increase of magnitude from 4.7 to 5.9 after the Tohoku earthquake (Uchida et al., 2015) and in Taiwan where the sequence of REs has a magnitude of 3.9 and 4.8 after a *M*6.9 nearby event (Chen et al., 2016). Thus, in this study, we do not impose any criterion on magnitude for grouping earthquakes into RE sequences. In Boso area, however, the magnitude of REs belonging to a same group does not vary much (see Figure S1 in the supporting information). We group together all pairs of REs that share a common earthquake on the sole basis of how their ruptures overlap. An example of a group of REs is shown in Figure 3.

The last stage of the preparation of the REs catalog consists in removing the doublets of REs. Doublets are REs that occur on the same asperity over a short time duration (typically a few hours). We suspect that the second doublet is in fact the aftershock of the first doublet (see Figure 10 of Lengliné & Marsan, 2009). The suppression of the doublet is conservative and does not create any artificial signal (see Figure S2 in the supporting information). The complete catalog (that includes the doublets is available in the supporting information).

3. Results

3.1. Repeating Earthquakes Analysis

The number of earthquakes in the JMA catalog (only magnitude ≥ 2 earthquakes are analyzed to have a complete catalog) increases during known SSEs (orange line in Figure 4), as well as a few days after the Tohoku-oki earthquake when a SSE also took place (Kato et al., 2014). These increases of the seismic activity correspond to the swarm-like seismicity that is concomittent with the SSEs (Hirose et al., 2012, 2014; Ozawa et al., 2003; Sagiya, 2004).

REs are also sensitive to the occurrence of nearby SSEs since their seismic rate increases during these slip episodes (blue line in Figure 4). Thus, we can use the REs as a proxy to assess changes in creeping rate on

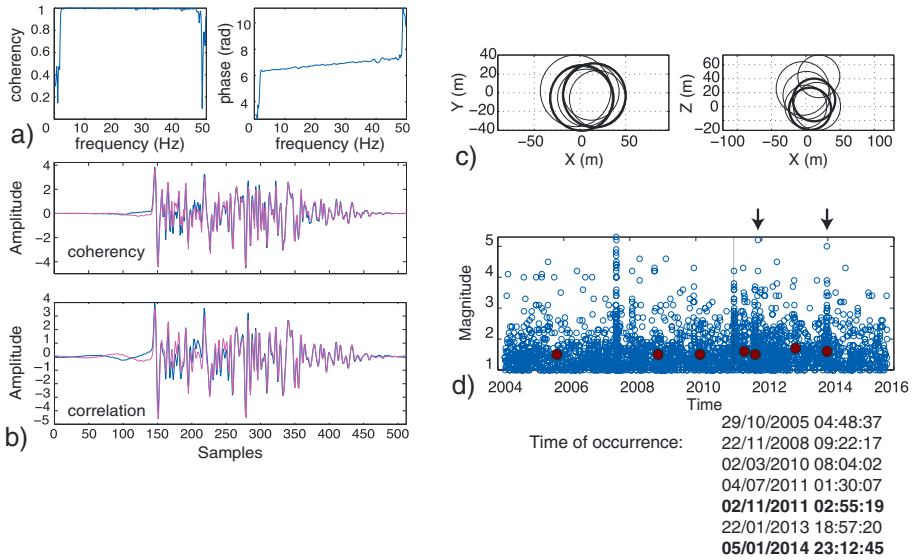

Figure 3. Example of the detection of a pair of repeating earthquakes. (a) Coherency and phase versus frequency. (b) Comparison of time-shifted waveforms, according to either the coherency or the correlation analysis at station CBAH. The slight difference between the two graphs is linked to a different smoothing used for correlation and coherency calculation. (c) Relative relocation of the two events in their RE group that counts seven occurrences. The two events of Figures 3a and 3b are shown with bold lines. (d) Time of occurrence of the events in this group; the two events of Figures 3a and 3b are shown with arrows along with all the 2,986 earthquakes analyzed here that are shown with blue dots. These two events occurred during two known SSEs (in 2011 and 2014). Times of occurrence of all the REs in the group are given; the bold ones indicate the two events of Figures 3a and 3b.

the subduction zone. With the method presented in section 2.2, we detect 308 REs with a total of 94 groups. Once we remove doublets, we are left with 202 REs. Additionally, the rate of REs shows two increases in 2005 and 2010. It is to be noted here that the swarm activity, triggered by the 2007, March 2011, and 2014 SSEs, is clearly visible on both the overall seismicity (orange line in Figure 4) and the RE activity (blue line). This is not the case for the 2005 and 2010 increases that can only be seen on the RE time series, which could explain why they have escaped detection so far, that is, when using the overall seismicity only to detect swarm-like seismicity. These are thus suspected, smaller instances of SSEs, that we further investigate now.

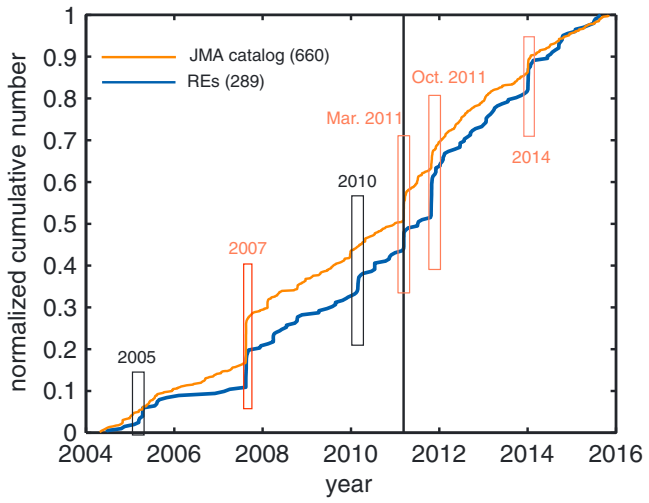

Figure 4. Normalized cumulative global seismicity in the Boso area (magnitude 2 and greater, in orange) and normalized cumulative number of REs (in blue). The total number is given in the brackets in the legend. The timing of known SSEs is shown with red rectangles and can clearly be seen in the raw seismicity and REs data. If an asperity is active several times during a known or suspected SSE, we kept only the biggest event of the group for generating these time series. The suspected SSEs in 2005 and 2010 are outlined with black lines and can only be seen on the repeating earthquake activity.

3.2. GPS Data Analysis.

In order to confirm the existence of such SSE, we analyzed the GPS times series projected in the direction N40°W. It evidences velocity variations accompanied by the occurrence of REs (Figure 5). Acceleration in the direction of the southeast is shown in red. For example, the 2007 SSE is clearly seen along with the concomitant swarm-like seismicity.

The GPS data clearly see a deformation transient in 2010 which maximum value is centered on the station 3033 and that activates all the stations used in this study (Figure 5). The direction of the deformation is coherent with the deformation of the 2007 SSE. However, it is still unclear why the geodetic transient precedes the burst of REs by about 2 months. This has, however, been seen elsewhere: the 2008 transient observed with pressure gauges by Ito et al. (2013) in the future rupture zone of the Tohoku earthquake was only followed 10 days later by a burst in seismicity.

In 2005, we note that a clear change in surface displacement rate concomitant with these 2005 bursts is mainly observed at station 3033 and small changes in displacement rate at stations 3027 and 3025 (Figure 5) so giving credence to a localized (rather than regional) transient deformation. However, the GPS velocity during the period of the first burst

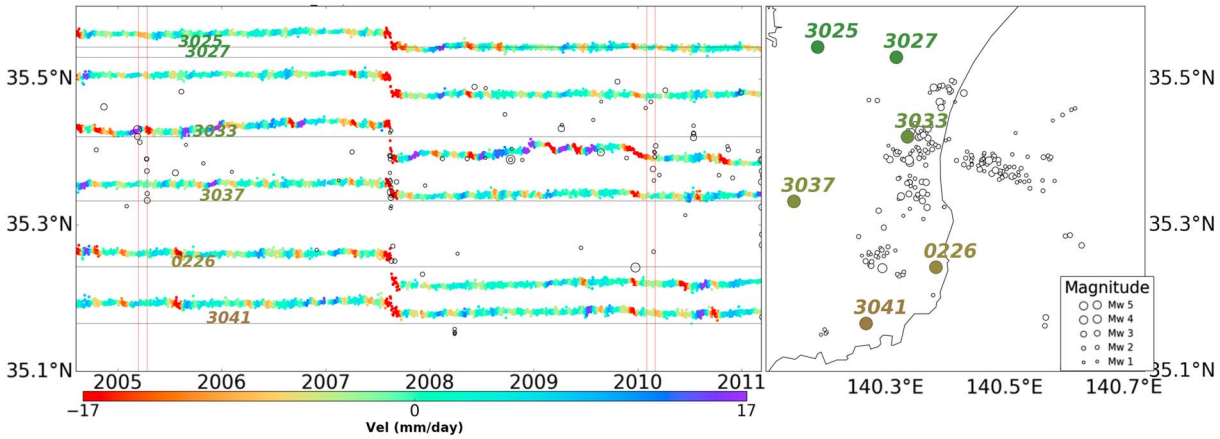

Figure 5. (left) Detrended position time series of GPS stations in Boso peninsula, projected in the direction N40°W (i.e., the azimuth of SSEs slip vectors). Colors show the variation of average GPS velocities computed in 1 month sliding windows. Stations are ordered as a function of the latitude. Circles indicate the locations and times of occurrence of REs. (right) Locations of GPS stations and REs. The two suspected SSEs in 2005 and 2010 are shown within vertical red lines.

(12 March 2005) is northwestward and southwestward during the second burst. Therefore, we assume that we reached the resolution limit of the GPS data analyses.

Other deformation transients are seen on stations 3033 in 2006, 2009, and 2010. This is also the case for stations 0226 and 3041 that record a transient at the same time in 2005. However, none of these transients are accompanied by an increase of REs seismicity as it is the case in 2005 and 2010. Furthermore, other changes in REs seismic rate are seen in Figure 4 with a smaller extent. We analyzed the smoothed rate of events over 10 days: for a time t, we count the number of events that occurred 5 days before and 5 days after and divide it by 10. The SSEs of 2005 and 2010 are still visible, and they are the highest peaks after the already known SSEs

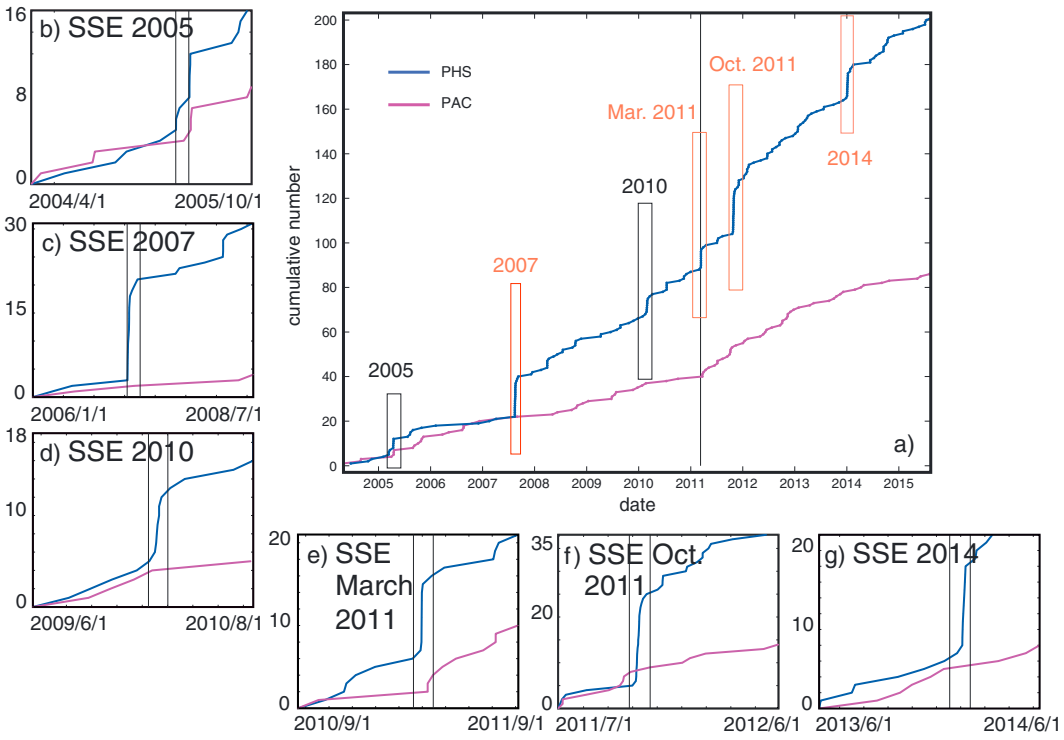

Figure 6. (a) Cumulative number of REs on PHS (blue) and on PAC (purple). (b–g) Zooms of cumulative number of REs for every SSEs are also displayed. The beginning and ending dates of the time axis are given. The time lag between the two vertical black lines corresponds to one month in all cases. This shows that the 2005 SSE has a longer duration than the others.

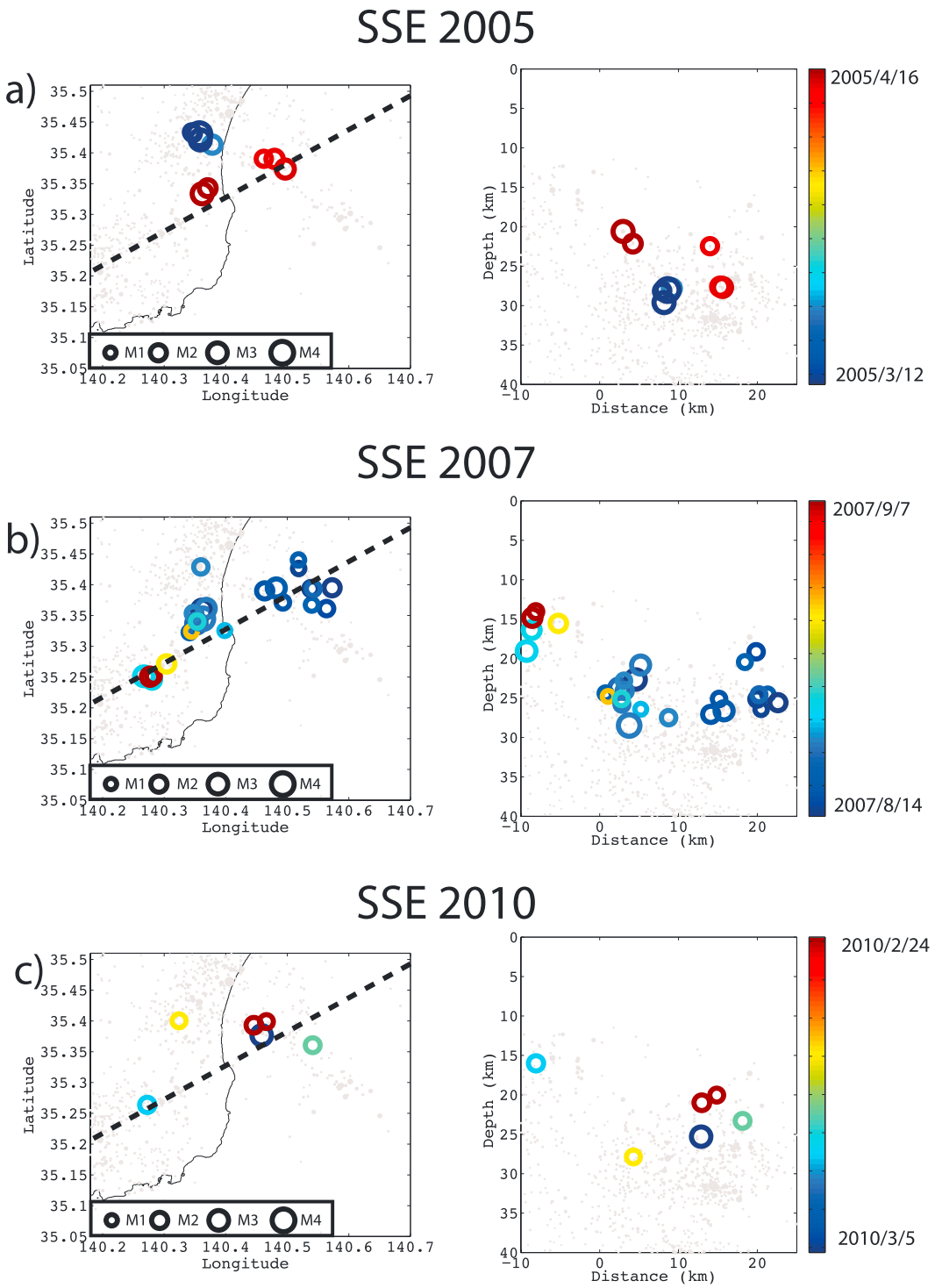

Figure 7. Location of the activated REs on a map and on an cross-section (only PHS is shown here since it hosts most of the REs), with the events projected on the dashed line which has an azimuth of 56°. The color code gives the time of occurrence during the SSEs for the 2005, 2007, and 2010 SSEs. The location error is the JMA catalog location error.

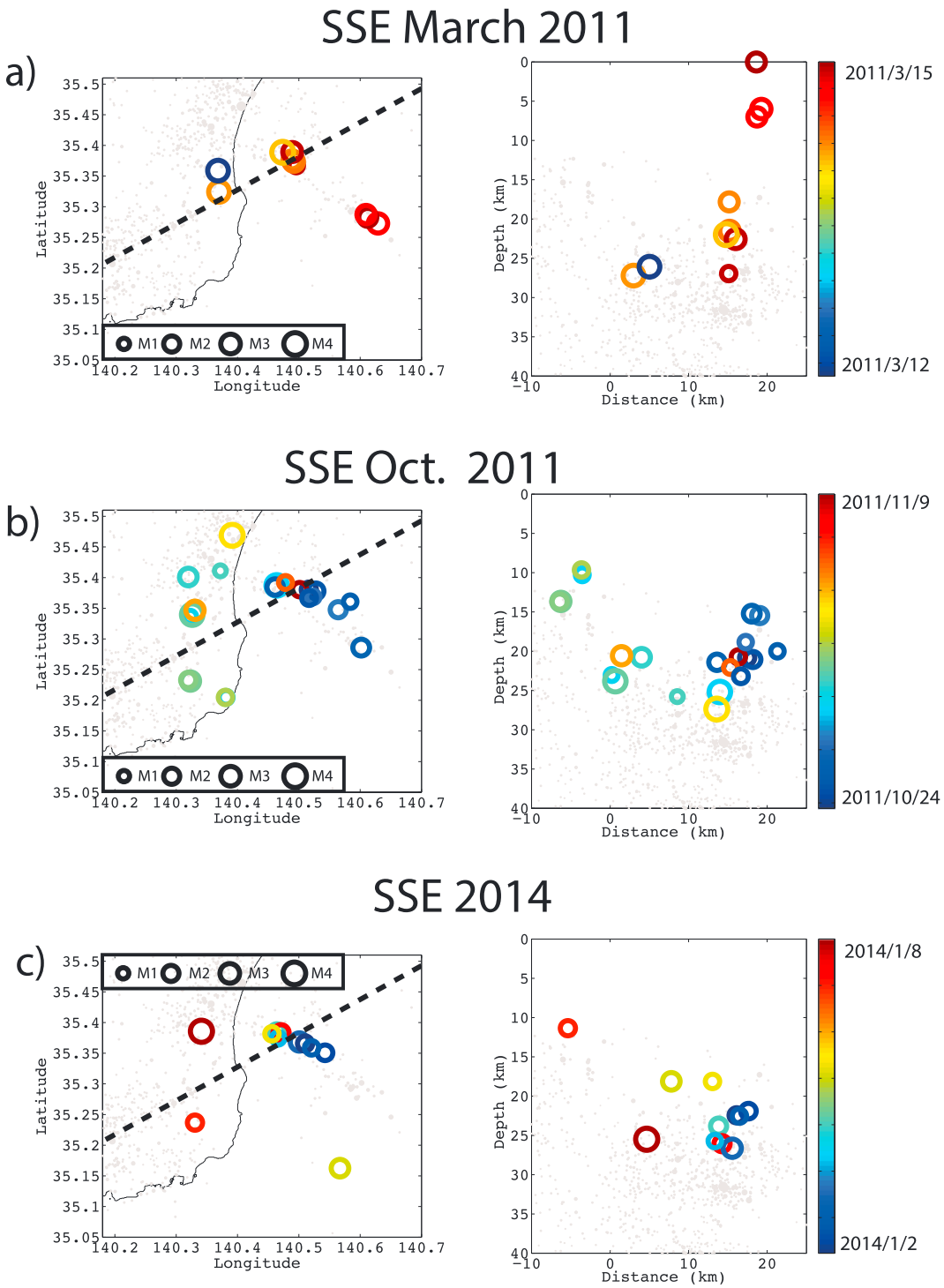

Figure 8. Same as 7 but for the March 2011, October 2011, and 2014 SSEs. The location error is the JMA catalog location error.

(see Figure S3 in the supporting information). Other peaks are still visible, and our assumption is that they are due to even smaller SSEs than the 2005 and 2010 ones. The deformation signal of the 2010 SSE is very clear and is concomitant with 9 REs, on the other hand, the deformation signal of the 2005 SSE is observed only at one station but is concomitant with 10 REs. Thus, the detection limit of the joint analysis of REs and GPS relies on the number of REs (typically less than 9) and the existence of a clear signal on the GPS data (the limit here is the 2005 SSE signal).

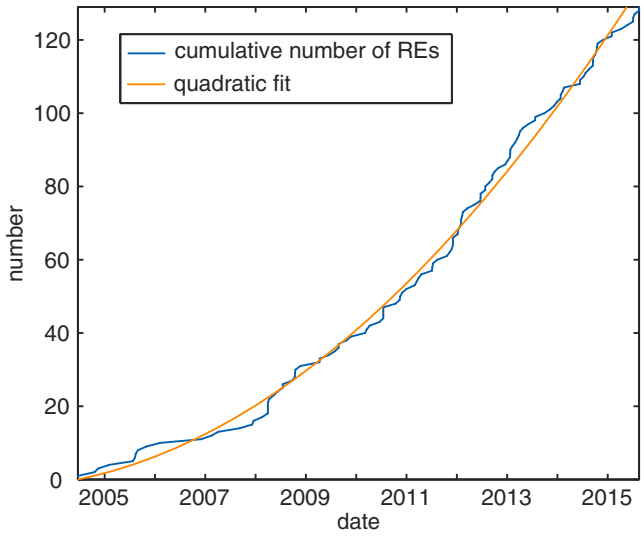

Figure 9. Normalized cumulative number of REs on PHS that did not occur during an SSE. The orange line indicates the quadratic fit applied on the data.

3.3. Slip Processes Analysis

In order to analyze in detail the SSEs slip processes seen by REs, we separate the groups of REs according to their depths (events shallower than 35 km belong to PHS and events deeper than 35 km belong to PAC see Figure S4 in the supporting information) to allocate them to PHS/OKH interface or PAC/PHS interface (PHS and PAC respectively, thereafter). For all geodetically resolved SSEs in our analysis period (in 2007, October 2011, and 2014), REs are almost only seen on PHS (Figure 6).

The episode of high rate in 2005 is made of two short bursts (Figure 6b), the first on 12 March 2005 (on PHS only) containing five REs and the second in 13 April 2005 also with five REs, and which is rapidly followed by a burst of three REs on PAC on 16 April 2005. A *M*6.1 earthquake struck on the 11 April 2005 in Choshi, at about 60 km to the north of Boso, on the PAC-OKH interface. This mainshock appears to have generated uplifts several times larger than expected for a normal *M*6.1 earthquake (Kobayashi & Hirose, 2016). It is therefore uncertain whether the second burst effectively results from slow slip originating from the usual Boso SSE patch, or from regional deformation accompanying or triggered by this *M*6.1 rupture. However, five $M \geq 6$ earthquakes occurred between 2005 and 2012, none of them triggering REs on PHS plate (Figure 1). Furthermore, no clear deformation is recorded at the station 3027 which is the station used in this study the closest to the event. Also, the seismicity declustering performed in Reverso et al. (2016) yields an increase in background rate in early 2005 (Figure S5 in the supporting information). Accounting for aftershock triggering and mean-field mechanical interaction laws does not suppress this anomalous seismicity transient, although its intensity is moderate. The REs that occurred from 12 March 2005 to 16 April 2005 are located first at depth on PHS and then migrate on both sides of the slipping patch (Figure 7a).

During the 2010 SSEs, nine REs occurred from the 24 February 2010 to the 5 March 2010, among which eight are on PHS, and only one is located on PAC (Figure 6d). The mean daily rate of REs on PHS is about 0.007/day for the periods without SSEs. Thus, the mean number of REs over 2.5 months is around 0.4, which is far from nine.

The REs history confirms previous observations on known SSEs. In 2007, the activated REs occur first on the eastern part of the PHS plate and migrate to the west (Figure 7b). This is coherent with the geodetic inversions of Hirose et al. (2014), where slip starts in the northeast part of the patch and migrates to the southwest. The maximum slip that occurred during the 2007 SSE estimated by Hirose et al. (2014) by inverting surface geodetic data was 250 mm, at 140.6° longitude and 35.05° latitude.

In March 2011, the 11 REs we found were activated during only 3 days from the 12 March 2011 to the 15 March 2011. The first REs occurred at depth (26 km) and the sequence then migrated toward shallower depths (20 to 5 km) along the eastern part of the fault plane (Figure 8a). The time series after the 2011 Tohoku-oki earthquake likely involves also a direct coseismic effect, as well as postseismic slip on PAC, so that the March 2011 SSE is mixed with high RE rates caused by more than local slip on the PHS-OKH interface. Since this slip event occurred only 4 days after the Tohoku-oki earthquake, it is thus impossible to invert the GPS data. However, the location and migration of the REs indicate that the slip probably had a smaller extension than the 2007 and 2010 SSEs and that it began at depth and migrated toward the surface.

In October 2011, the entire area surrounding the patch was seismically activated. As for the 2007 SSE, it started on the eastern branch of the fault and migrated to the west while activity on the eastern branch was still ongoing (Figure 8b). It is also coherent with the work of Hirose et al. (2014): they estimated a maximum slip of 300 mm centered at 140.5° longitude and 35.05° latitude, that is, more to the west than the maximum slip of the 2007 SSE.

In 2014, the initiation of the REs is delayed compared to the onset of the slow slip which started on the 28 December 2013. The sequence started on the eastern part of the fault, as REs are mainly observed in this area (Figure 8c). Two other REs occurred on the western and deeper part of the fault, and an additional one is found inside the slipping fault patch. This is in good agreement with the slip distribution estimated by Ozawa (2014). During this SSE, the slip occurred farther away from the coast than during the 2007 and

Table 1
Displacements (in mm), Seismic Moment, and Magnitudes Estimated for the SSEs Using Nadeau and Johnson's Relationship (Nadeau & Johnson, 1998) on REs That Occurred During the Transient Events

SSE	Cumulative slip (mm)	Mo (N m)	Magnitude	Magnitude from GPS data	Reference
2005	8.9	9.97×10^{17}	5.9 (from REs)	~5.8	This study
2007	18.4	2.06×10^{18}	6.1	6.6	Ozawa et al. (2007)
2010	8.6	9.63×10^{17}	5.9 (from REs)	~6.1	This study
March 2011	12.9	1.45×10^{18}	6.0	<6.5 ?	Kato et al. (2014)
October 2011	23.7	2.65×10^{18}	6.2	6.6	Hirose et al. (2012)
2014	10.9	1.23×10^{18}	6.0	6.5	Ozawa (2014)

Note. These estimated moment magnitude obtained in this study, and only based on REs time series, are compared to the estimated ones from GPS (last two columns).

October 2011 SSEs. The total slip amount for this SSE is 10 cm. It had a magnitude of M_w6.5 which is slightly smaller than those of 2007 and October 2011 that had a M_w6.6 (Hirose et al., 2014; Ozawa, 2014; Ozawa et al., 2007). The spatiotemporal evolution of this SSE can be divided in two phases (Fukuda et al., 2014). The first phase (from 1 to 30 2013) corresponds to a small slow slip event that begins offshore and that slowly migrates to the west. The second phase (from the 30 December 2013 to 9 January 2014) shows a rapid slip acceleration while the westward migration still continued. The REs that we evidence occurred during this second phase only.

3.4. Inter-SSE REs Analysis

The analysis of the cumulative number of REs on PHS that did not occur during an SSE indicates that an increase of the seismic rate has been taking place since 2005 in this area (Figure 9). This suggests that the coupling is progressively reducing with time and that, beside the SSEs, a long-term transient is taking place which is coherent with the acceleration of background seismicity reported in Reverso et al. (2016) for the Boso area, 1990–2015. This is in good agreement with the increase of the background seismicity in an area located offshore Boso (area G in Figure 6 of Marsan et al., 2017).

3.5. Seismic Moment Estimation of the SSEs

We estimate the seismic moment of the SSEs using equation (1):

$$\log(d) = -3.17 + 0.17 \log(M_o) \quad (1)$$

that relates the seismic moment (M_o in N m) with the slip (d in m). This empirical relationship has been used in Japan for estimating slip from RE time series (Igarashi et al., 2003; Uchida et al., 2003, 2009). The results are shown in Table 1.

While it is unclear why this law would hold in Boso, as well as the rest of the Japanese subduction zone, we make use of it as a way to estimate the sizes of the 2005 and 2010 SSE relative to the 2007, October 2011, and 2014 SSEs, for which moments are directly known from GPS observations.

We thus calculate the cumulative slip taking into account the events that occurred during a SSE. Once we obtain the cumulative aseismic slip of each SSE using Nadeau and Johnson relationship, we use the proportionality with the value of the 2007 SSE seismic moment to avoid an estimation of the slip area. Although the use of cumulative slip seems to underestimate M_o compared to previous studies, it yields a first estimation of the maximum value of M_o for the SSEs suggested by our analysis.

The use of Nadeau and Johnson (1998) relationship gives a seismic moment of 9.97×10^{17} N m (M_w = 5.9) and 9.63×10^{17} N m (M_w=5.9) for the 2005 and 2010, respectively.

Another approach to estimate the M_o is the use of the displacement value recorded on GPS data. The analysis of the displacements at the GPS

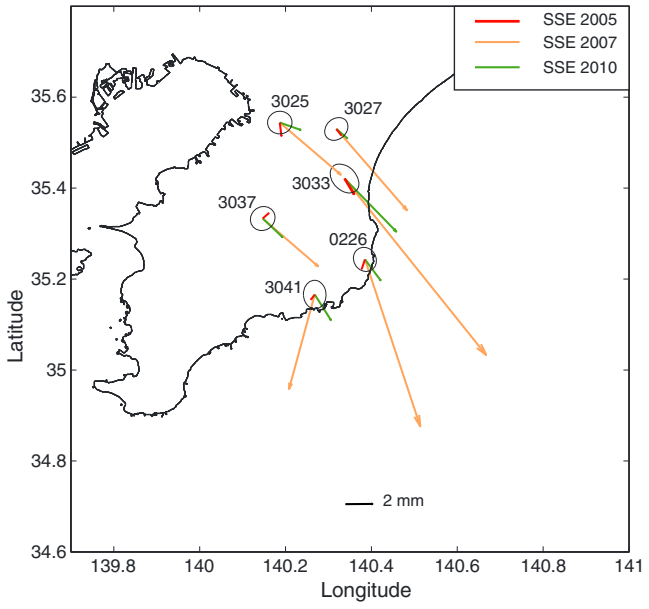

Figure 10. Displacements due to the 2005 (red), 2007 (orange), and 2010 (green) SSEs, in mm. The black ellipses show the noise level estimated by an analysis on the principal component during the year 2006 when no SSEs occurred.

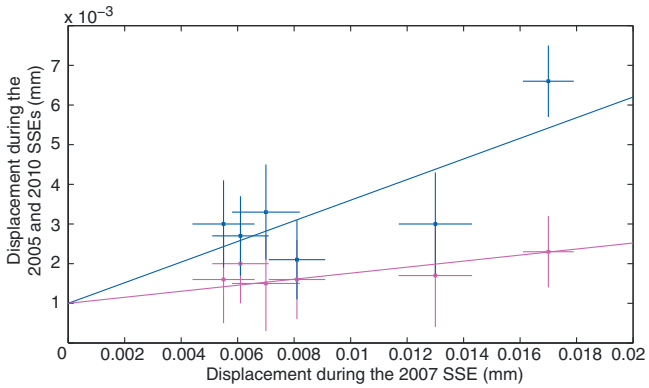

Figure 11. Displacement during the 2005 (purple) and the 2010 (blue) SSEs versus displacement during the 2007 SSE. The error bars show the noise level in the data estimated by the analysis of the GPS data in 2006. The line indicates the affine function defined in the text.

stations shows that their directions are coherent between the 2007 and the 2010 SSEs (Figure 10). This observation confirms the displacements observed in Figure 5 and the clear occurrence of a SSE in 2010. Concerning the 2005 SSE, the displacement recorded at station 3033 is still clear but just out of the noise level represented here by black ellipses. The displacements recorded at the other stations are, however, under the noise level. It confirms that with this event, we are at the limit of the resolution of the SSE detection.

Given that the directions of displacement are coherent, we can hypothesize that slip takes place on the same patch so that the seismic moment is proportional to the surface displacement at the stations.

To estimate the magnitude of the 2010 SSE, we thus fit the values of the displacement due to the 2010 SSE versus the displacement due to the 2007 SSE with an affine function: $d_{2010} = d_{2007} \times x$; the least squares estimate gives $x = \overline{d_{2010} d_{2007}} / \overline{d_{2007}^2}$ with $\overline{}$ denoting the mean over the stations (Figure 11). We first estimate the noise level. To do so, we analyze the GPS signal during 2006, when no SSEs occurred, and calculate the covariance of the displacement of the north-south and east-west components. Then, we compute the mean of the eigenvalues of the covariance to estimate the noise level. We add a Gaussian noise to the GPS signal based on the noise level previously computed and estimate the value of x. We find a value of $x = 0.26 \pm 0.04$. This gives a difference in magnitude from −0.44 to −0.5. Thus, according to this computation, the moment magnitude of the 2010 SSE is about 6.1. We did the same calculation for the 2005 SSE but since the signal is smaller, the relative uncertainty is 50%: $x = 0.076 \pm 0.04$. This gives a moment magnitude of about 5.8.

The 2005 and 2010 SSEs both present smaller magnitudes than the already known SSEs, which explains why they are not as easily observed in geodetic data as the bigger SSEs. Furthermore, they show uncharacteristic behaviors in the timing of activation of the REs compared to the SSEs occurrence time. The estimation of the magnitudes using REs and GPS data gives similar results, showing that the REs analyzed in this study are likely linked to the occurrence of SSEs, but we are at the edge of the resolution limit concerning the 2005 SSE.

4. Discussion

In several tectonic regions of the world, slow slip episodes are known to occur along with seismic tremors. The latter is seen as the repetitive rupture of very small asperities, hence a by-product of slow slip. Tremors allow to detect and track slow slip events well below the resolving power of GPS stations. Swarms of tremors over a continuum of sizes have indeed been observed, in Cascadia, from M_w5 (undetected by GPS stations) to M_w6.7, these sizes following the equivalent of a Gutenberg-Richter law (Wech et al., 2010). Bursts of low-frequency earthquakes in the Mexican subduction zone have been shown to accompany slow slip, which can be resolved from GPS signals by stacking over many bursts (Frank et al., 2015; Frank, 2016). In both the Cascadia and Mexico cases, the size distribution of slow slip events as monitored by tremors or low-frequency earthquakes appears to be depth dependent, with only the largest slip events reaching the uppermost part of the transition zone (Wech & Creager, 2011).

Boso slow slip events (SSEs) do not trigger seismic tremors, possibly owing to their shallow depth (Delahaye et al., 2009) and/or their short duration, hence their (relatively, for SSEs) large slip rate (Montgomery-Brown & Syracuse, 2015). It is thus more difficult to detect smaller instances of slow slip. Instead of tremors, earthquake swarms mark the occurrence of SSEs there. So far, the geodetically known SSEs in Boso have characteristic sizes (M_w6.5 to 6.7) and duration (about 1 week), but the question remains as to the existence of smaller SSEs below this characteristic size, and their occurrence rates, especially in this area that has been undergoing a long-term (20 year long) acceleration of activity (Figure 9, Marsan et al., 2017; Reverso et al., 2016).

Deciphering seismicity rates to identify possible episodes of slow slip is, however, not trivial, since transient increases in rate can also be triggered by local mainshocks. Reverso et al. (2016) separated the aftershock rate from the so-called background rate, for $m \geq 2.0$ earthquakes, and proposed that, at first order, the change in background rate during an SSE is directly proportional to its seismic moment. Isolating smaller SSEs

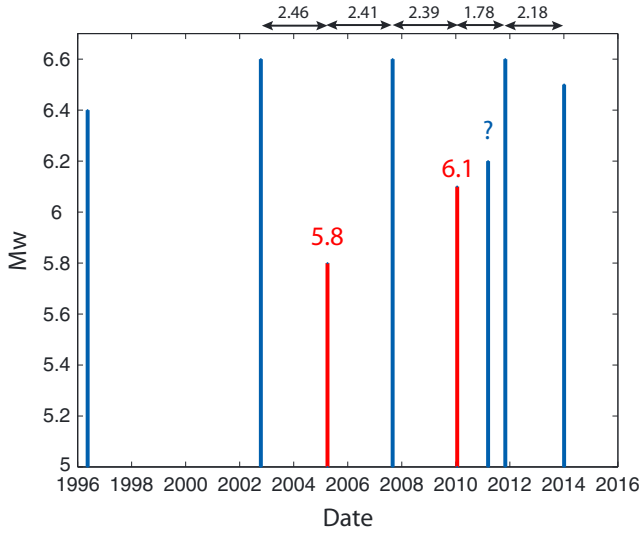

Figure 12. Updated history of the Boso SSEs showing the two hidden SSEs that occurred in 2005 and 2010. We estimated their magnitude using GPS data. Magnitude of already known SSEs were determined by Hirose et al., 2014 (2014), Ozawa et al., 2003 (2003, 2007), Ozawa, (2014), and Sagiya, (2004). The magnitude of March 2011 SSE was estimated smaller than 6.5 (Kato & Nakagawa, 2014). Time in years between two successive SSEs is given on the top.

would then imply finding other statistically significant background rate increases, using smaller magnitude earthquakes (i.e., well below $m = 2$).

This has been performed by Kato et al. (2014) who used a template matching method, for a 1 month long period containing the date of the 2011 Tohoku earthquake, to discover a SSE not resolvable by GPS (due to ongoing afterslip) with a smaller size than the characteristic size, starting 1 day after the mainshock. A systematic search for seismicity bursts unrelated with aftershock sequences remains to be performed over an extended period of time at small magnitude at Boso. We here searched for repeating earthquakes over the 2004–2015 interval. The similarity of the waveforms suggests that these earthquakes rupture the same asperity, which must be relatively isolated from neighboring asperities, and thus less sensitive to mechanical interactions (stress transfer) from local earthquakes. The two largest rate increases of repeating earthquakes (with magnitudes $m \geq 1.0$) over one to several weeklong periods, outside the already known SSEs, correspond to two events in 2005 and 2010, both having signatures in the GPS signals, at least for the closest station (3033).

The fact that the 2005 SSE presents a smaller magnitude and/or lateral extension and that the 2010 SSE lasts longer than the already known SSE strongly suggest that the fault plane of the Boso SSE has a complex slip history. Furthermore, the 2014 SSE has a nucleation phase (Fukuda et al., 2014) which could also be the case for previous SSEs, in which case we should distinguish the "seismic" duration from the "slip" duration. This also characterizes well the behavior of the 2010 SSE that started to slip before the seismicity started. The RE activity is more intermittent for the 2005 SSE compared to the shorter (known) SSEs, to the extent that it becomes somewhat arbitrary to group the two observed bursts in one single SSE. Instead, slip could be having several phases of acceleration/stopping (or deceleration), equivalent to as many (smaller) SSEs.

Models exist that relate RE occurrence with slow slip, typically using rate-and-state friction modeling, with REs corresponding to the ruptures of velocity-weakening, isolated patches (i.e., density of patches is below a critical density), on an otherwise creeping fault (Dublanchet et al., 2013). These studies show that the rate of occurrence of REs is a direct measure of the creep rate. For patch density above the critical density, the behavior is certainly more complex, but then ruptures extend over (seemingly) random numbers of neighboring patches, so that the seismic source are not similar anymore. We thus do not believe this situation arises in our study since we focus on highly similar sources.

Recent laboratory study on slow earthquakes behaviors show that the duration of such events depends on the effective stiffness of the fault (Leeman et al., 2016). Another explanation of the difference in slipping extension is the variation of stress state with time. The frictional parameters and stress state may vary with time on the SSE fault plane explaining why the extensions can be different from one SSE to another. Also, since the portion at greater depth is at higher temperature, it might be more sensitive to pore fluid pressure variation which directly has an effect on the stress state and the ability to reach a slip-weakening regime. Such variations of slow slip extension were recorded in the Cascadia subduction zone at a greater lateral extension since the episodic tremors and slip events (ETS) cover several hundreds of kilometers (Brudzinski & Allen, 2007; Wech & Bartlow, 2014). On the contrary, in Bungo Channel area, the slip distributions of the three long-term slow slip events of 1997, 2003, and 2010 present a different history but covers the same plate interface (Yoshioka et al., 2015).

5. Conclusion

In this study, thanks to the joint analysis of REs and GPS data, we are able to detect two SSEs during a time span that counted four previously known SSEs. Both GPS and REs signals are clear for the 2010 SSE. In 2005, the REs time series evidence a change in the REs seismic rate concomitant with a much less clear change in displacement in the GPS data. We therefore conclude that the resolution limit of the method is reached for the 2005 SSE. They show different slip extensions and different magnitudes than the already known SSEs.

This leads to a totally new history of the slip in the area (Figure 12). In between 2003 and the Tohoku earthquake, the SSEs occurred every 2.4 years on a regular basis, instead of the 6–7 years previously estimated. There is no clear evidence of unknown SSE between the March 2011 and the 2014 SSEs which is probably due to the fact that the time interval between SSEs has been decreasing, due to the Tohoku earthquake (Hirose et al., 2012; Kato & Nakagawa, 2014). Without taking the March 2011 into account, we see that the regularity of the time of occurrence is rather well preserved. This might indicate the possible occurrence of a SSE in the end of 2016 to the beginning of 2017. This study raises several questions: are all displacements anomalies recorded in the GPS data due to even smaller SSEs? Are all SSEs linked to the change of the background seismicity? Or to the occurrence of REs? Going deeper in the signals and pushing the resolution limit will certainly bring new answers. In order to properly assess the Boso slip history since the 1990s, the same analysis on REs and GPS data can be done over the period 1990–2004.

Acknowledgments
Earthquake data and the JMA catalog were kindly provided by the Japan Meteorological Agency in cooperation with the Ministry of Education, Culture, Sports, Science, and Technology. We acknowledge the help of the National Research Institute for Earth Science and Disaster Prevention, Tsukuba, for making available their waveform data through their website. This work has been supported by a grant from LabEx Osug@2020 (ANR10LABX56) and by the European Union's Horizon 2020 research and innovation program EPOS-IP (676564). Most of the computations presented in this paper were performed using the CIMENT infrastructure (https://ciment.ujf-grenoble.fr), which is supported by the Rhone-Alpes region (grant CPER07_13 CIRA: http://www.ci-ra.org) and France-Grille (http://www.france-grilles.fr). We are thankful to B. Bzeznik and F. Roch. We would like to thank two anonymous reviewers and the Associate Editor for their help in improving this manuscript.

References

Altamimi, Z., Rebischung, P., Métivier, L., & Collilieux, X. (2016). ITRF2014: A new release of the International Terrestrial Reference frame modeling nonlinear station motions. *Journal of Geophysical Research: Solid Earth*, *121*, 6109–6131. https://doi.org/10.1002/2016JB013098

Boehm, J., Werl, B., & Schuh, H. (2006). Troposphere mapping functions for GPS and very long baseline interferometry from European Centre for Medium-Range Weather Forecasts operational analysis data. *Journal of Geophysical Research*, *111*, B02406. https://doi.org/10.1029/2005JB003629

Bouchon, M., Karabulut, H., Aktar, M., Ozalaybey, S., Schmittbuhl, J., & Bouin, M. (2011). Extended nucleation of the 1999 M_w 7.6 Izmit earthquake. *Science*, *331*, 877–880.

Brudzinski, M., & Allen, R. (2007). Segmentation in episodic tremor and slip all along Cascadia. *Geology*, *35*, 907–910.

Chen, K., Nadeau, R., & Rau, R.-J. (2007). Towards a universal rule on the recurrence interval scaling of repeating earthquakes? *Geophysical Research Letters*, *34*, L16308. https://doi.org/10.1029/2007GL030554

Chen, K., Chen, I., & Kim, A. (2016). Can slip heterogeneity be linked to earthquake recurrence? *Geophysical Research Letters*, *43*, 6916–6923. https://doi.org/10.1002/2016GL069516

Delahaye, E. J., Townend, J., Reyners, M. E., & Rogers, G. (2009). Microseismicity but no tremor accompanying slow slip in the Hikurangi subduction zone, New Zealand. *Earth and Planetary Science Letters*, *277*, 21–28.

Dublanchet, P., Bernard, P., & Favreau, P. (2013). Interactions and triggering in a 3-D rate-and-state asperity model. *Journal of Geophysical Research: Solid Earth*, *118*, 2225–2245. https://doi.org/10.1002/jgrb.50187

Ellsworth, W. L., & Beroza, G. (1995). Seismic evidence for an earthquake nucleation phase. *Science*, *268*, 851–855.

Eshelby, J. (1957). The determination of the elastic field of an ellipsoidal inclusion, and related problems. *Proceedings of the Royal Society of London Series A*, *241*, 376–396.

Frank, W. B. (2016). Slow slip hidden in the noise: The intermittence of tectonic release. *Geophysical Research Letters*, *43*, 10,125–10,133. https://doi.org/10.1002/2016GL069537

Frank, W. B., Radiguet, M., Rousset, B., Shapiro, N. M., Husker, A. L., Kostoglodov, V., … Campillo, M. (2015). Uncovering the geodetic signature of silent slip through repeating earthquakes. *Geophysical Research Letters*, *42*, 2774–2779. https://doi.org/10.1002/2015GL063685

Fukuda, J., Kato, A., Obara, K., & Miura, S. (2014). Imaging of the early acceleration phase of the 2013–2014 Boso slow slip event. *Geophysical Research Letters*, *41*, 7493–7500. https://doi.org/10.1002/2014GL061550

Gardonio, B., Marsan, D., Lengliné, O., Enescu, B., Bouchon, M., & Got, J. (2015). Changes in seismicity and stress loading on subduction faults in the Kanto region, Japan, 2011–2014. *Journal of Geophysical Research: Solid Earth*, *120*, 2616–2626. https://doi.org/10.1002/2014JB011798

Got, J., Fréchet, J., & Klein, F. (1994). Deep fault plane geometry inferred from multiplet relative relocation beneath the south flank of Kilauea. *Journal of Geophysical Research*, *99*, 15,375–15,386.

Got, J.-L., & Okubo, P. (2003). New insights into Kilauea's volcano dynamics brought by large-scale relative relocation of microearthquakes. *Journal of Geophysical Research*, *108*(B7), 2553. https://doi.org/10.1029/2002JB002060

Herring, T. A., King, R. W., & McClusky, S. C. (2010). *Introduction to Gamit/Globk*. Cambridge, MA: Massachusetts Institute of Technology.

Hirose, H., Kimura, H., Enescu, B., & Aoi, S. (2012). Recurrent slow slip event likely hastened by the 2011 Tohoku earthquake. *Proceedings of the National Academy of Sciences of the United States of America*, *109–38*, 15,157–15,161.

Hirose, H., Matsuzawa, T., Kimura, T., & Hisanori, K. (2014). The Boso slow slip events in 2007 and 2011 as a driving process for the accompanying earthquake swarm. *Geophysical Research Letters*, *41*, 2778–2785. https://doi.org/10.1002/2014GL059791

Igarashi, T., Matsuzawa, T., & Hasegawa, A. (2003). Repeating earthquakes and interplate aseismic slip in the northeastern Japan subduction zone. *Journal of Geophysical Research*, *108*, 2249. https://doi.org/10.1029/2002JB001920

Ishida, M. (1992). Geometry and relative motion of the Philippine Sea plate and Pacific plate beneath the Kanto-Tokai District, Japan. *Journal of Geophysical Research*, *97*(B1), 489–513.

Ito, Y., Hinoa, R., Kidob, M., Fujimotob, H., Osadab, Y., Inazuc, D., … Ashi, J. (2013). Episodic slow slip events in the Japan subduction zone before the 2011 Tohoku-Oki earthquake. *Tectonophysics*, *600*, 14–26.

Kato, A., & Nakagawa, S. (2014). Multiple slow-slip events during a foreshock sequence of the 2014 Iquique, Chile M_w 8.1 earthquake. *Geophysical Research Letters*, *41*, 5420–5427. https://doi.org/10.1002/2014GL061138

Kato, A., Igarashi, T., & Obara, K. (2014). Detection of a hidden Boso slow slip event immediately after the 2011 M_w 9.0 Tohoku-Oki earthquake, Japan. *Geophysical Research Letters*, *41*, 5868–5874. https://doi.org/10.1002/2014GL061053

Kimura, H., Kasahara, K., Igarashi, T., & Hirata, N. (2006). Repeating earthquake activities associated with the Philippine Sea plate subduction in the Kanto district, central Japan: A new plate configuration revealed by interplate aseismic slips. *Tectonophysics*, *417*, 101–118.

Kobayashi, A., & Hirose, F. (2016). *Aseismic slips synchronized with earthquakes in northern Chiba Prefecture, Central Japan*, *69*(2), 1–9.

Leeman, J., Saffer, D., Scuderi, M., & Marone, C. (2016). Laboratory observations of slow earthquakes and the spectrum of tectonic fault slip modes. *Nature Communications*, *7*, 11104.

Lengliné, O., & Marsan, D. (2009). Inferring the coseismic and postseismic stress changes caused by the 2004 $Mw = 6$ Parkfield earthquake from variations of recurrence times of microearthquakes. *Journal of Geophysical Research*, *114*, B10303. https://doi.org/10.1029/2008JB006118

Lomax, A., Michelini, A., & Curtis, A. (2009). Earthquake location, direct, global-search methods.
Lyard, F., Lefevre, F., Letellier, T., & Francis, O. (2006). Modelling the global ocean tides: A modern insight from FES2004. *Ocean Dynamics*, *56*, 394–415.
Marsan, D., Bouchon, M., Gardonio, B., Perfettini, H., Socquet, A., & Enescu, B. (2017). Change in seismicity along the Japan trench, 1990–2011, and its relationship with seismic coupling. *Journal of Geophysical Research: Solid Earth*, *122*, 4645–4659. https://doi.org/10.1002/2016JB013715
Matsuzawa, T., Igarashi, T., & Hasegawa, A. (2002). Characteristic small-earthquake sequence off Sanriku, northeastern Honshu, Japan. *Geophysical Research Letters*, *29*(11), 1543. https://doi.org/10.1029/2001GL014632
Matsuzawa, T., Hirose, H., Shibazaki, B., & Obara, K. (2010). Modeling short- and long-term slow slip events in the seismic cycles of large subduction earthquakes. *Journal of Geophysical Research*, *115*, B12301. https://doi.org/10.1029/2010JB007566
Mitsui, Y. (2015). Interval modulation of recurrent slow slip events by two types of earthquake loading. *Earth, Planets and Space*, *67*, 56.
Montgomery-Brown, E., & Syracuse, E. M. (2015). Tremor-genic slow slip regions may be deeper and warmer and may slip slower than non-tremor-genic regions. *Geochemistry, Geophysics, Geosystems*, *16*, 3593–3606. https://doi.org/10.1002/2015GC005895
Nadeau, R., & Johnson, L. (1998). Seismological studies at Parkfied VI: Moment release rates and estimates of source parameters for small repeating earthquakes. *Bulletin of the Seismological Society of America*, *88*(3), 790–814.
Nadeau, R., & McEvilly, T. V. (1999). Fault slip rates at depth from recurrence intervals of repeating microearthquakes. *Science*, *285*, 718–721.
Nadeau, R. M., Foxall, W., & McEvilly, T. V. (1995). Clustering and periodic recurrence of microearthquakes on the San Andreas fault at Parkfield, California. *Science*, *267*, 503–507.
Ozawa, S. (2014). Shortening of recurrence interval of Boso slow slip events in Japan. *Geophysical Research Letters*, *41*, 2762–2768. https://doi.org/10.1002/2014GL060072
Ozawa, S., Miyazaki, S., Hatanaka, Y., Imakiire, T., Kaidzu, M., & Murakami, M. (2003). Characteristic silent slip earthquakes in the eastern part of the Boso peninsula, Central Japan. *Geophysical Research Letters*, *30*(6), 1283. https://doi.org/10.1029/2002GL016665
Ozawa, S., Suito, H., & Tobita, M. (2007). Occurrence of quasi-periodic slow-slip off the east coast of the Boso peninsula, Central Japan. *Earth Planets Space*, *59*, 1241–1245.
Reverso, T., Marsan, D., Helmstetter, A., & Enescu, B. (2016). Background seismicity in Boso Peninsula, Japan: Long-term acceleration, and relationship with slow slip events. *Geophysical Research Letters*, *43*, 5671–5679. https://doi.org/10.1002/2016GL068524
Sagiya, T. (2004). Interplate coupling in the Kanto District, Central Japan, and the Boso Peninsula Silent Earthquake in May 1996. *Pure and Applied Geophysics*, *161*, 2317–2342.
Schaff, D. P., Beroza, G. C., & Shaw, B. E. (1998). Postseismic response of repeating aftershocks. *Geophysical Research Letters*, *25*(24), 4549–4552.
Socquet, A., Valdes, J., Jara, J., Cotton, F., Walpersdorf, A., Cotte, N., … Norabuena, E. (2017). An 8 month slow slip event triggers progressive nucleation of the 2014 Chile megathrust. *Geophysical Research Letters*, *44*, 4046–4053. https://doi.org/10.1002/2017GL073023
Tu, Y., & Heki, K. (2014). The variations of long time period slow slip events along the Ryukyu subduction zone (American Geophysical Union Fall meetings), San Francisco.
Uchida, N., Matsuzawa, T., & Hasegawa, A. (2003). Interplate quasi-static slip off Sanriku, NE Japan, estimated from repeating earthquakes. *Geophysical Research Letters*, *30*, 1801. https://doi.org/10.1029/2003GL017452
Uchida, N., Nakajima, J., Hasegawa, A., & Matsuzawa, T. (2009). What controls interplate coupling?: Evidence for abrupt change in coupling across a border between two overlying plates in the NE Japan subduction zone. *Earth and Planetary Science Letters*, *283*, 111–121. https://doi.org/10.1016/j.epsl.2009.04.003
Uchida, N., Shimamura, K., Matsuzawa, T., & Okada, T. (2015). Postseismic response of repeating earthquakes around the 2011 Tohoku-oki earthquake: Moment increases due to fast loading rate. *Journal of Geophysical Research: Solid Earth*, *120*, 259–274. https://doi.org/10.1002/2013JB010933
Ukawa, M., Ishida, M., Matsumura, S., & Kasahara, K. (1984). Hypocenter determination method of the Kanto-Tokai observational network for microearthquakes. *Research Notes National Research Centre Disaster Prevention*, *53*, 1–88.
Wech, A., & Bartlow, N. (2014). Slip rate and tremor genesis in Cascadia. *Geophysical Research Letters*, *41*, 392–398. https://doi.org/10.1002/2013GL058607
Wech, A., & Creager, K. C. (2011). A continuum of stress, strength and slip in the Cascadia subduction zone. *Nature Geosciecnce*, *4*, 624–628.
Wech, A., Creager, K. C., Houston, H., & Vidale, J. E. (2010). An earthquake-like magnitude-frequency distribution of slow slip in northern Cascadia. *Geophysical Research Letters*, *37*, L22310. https://doi.org/10.1029/2010GL044881
Yoshioka, S., Matsuoka, Y., & Ide, S. (2015). Spatiotemporal slip distributions of three long-term slow slip events beneath the Bungo Channel, southwest Japan, inferred from inversion analyses of GPS data. *Geophysical Journal International*, *201*(3), 1437–1455.